ISSN 0965-5441, Petroleum Chemistry, 2019, Vol. 59, No. 9, pp. 1009–1016. © Pleiades Publishing, Ltd., 2019.
Russian Text © The Author(s), 2019, published in Neftekhimiya, 2019, Vol. 59, No. 5, pp. 560–568.

Ethylene Hydroformylation in the Presence of Rhodium Catalysts in Hydrocarbon-Rich Media: The Stage of Combined Conversion of Refinery Gases to Oxygenates

D. N. Gorbunov[a, *], M. V. Nenasheva[a], R. P. Matsukevich[a], M. V. Terenina[a], F. N. Putilin[a], Yu. S. Kardasheva[a, *], A. L. Maksimov[b], and E. A. Karakhanov[a]
[a]Faculty of Chemistry, Moscow State University, Moscow, 119234 Russia
[b]Topchiev Institute of Petrochemical Synthesis, Russian Academy of Sciences, Moscow, 119991 Russia
**e-mail: suskab_91@mail.ru*

Received March 14, 2019; revised May 10, 2019; accepted May 13, 2019

Abstract—The feature of hydroformylation of model gas mixtures with different ethylene, hydrogen, and methane concentrations in the presence of rhodium catalysts have been studied. The effect of the initial pressure in the reactor and the reaction temperature on the reaction rate and selectivity has been determined. It has been shown that ethylene hydroformylation occurs with a high propanal selectivity (up to 99%), with the turnover frequency of the reaction reaching 9500 h^{-1}. It has been proposed that various phosphine ligands should be used to implement alternative methods of separating the catalyst system from the reaction products.

Keywords: cracked gases, ethylene, methane, hydroformylation, oxygenates, fuel additives, oxygen-containing products, propanal, phosphine ligands, catalyst recycling

DOI: 10.1134/S0965544119090056

INTRODUCTION

Deep conversion of fossil hydrocarbons (HCs) is still an issue of current concern. At oil refineries equipped with HC cracking units, a significant amount of ethylene and saturated C_2+ gases is formed in addition to target commercial products; most commonly, these gases are combusted to generate heat [1–5]. This utilization cannot be considered rational, taking into account the large number of purification and preparation stages (drying, desulfurization) to which the feedstock is subjected and the low heat output during the combustion of mixtures of this composition [6]. Currently, methods to convert light HCs to high value-added products, such as oxygenates, are being actively searched for. Integration of gas conversion with the currently available production processes will make it possible to increase the feedstock conversion depth, improve the economic indicators of production, and expand the range of products manufactured by the enterprises.

Catalytic cracker gases can contain a certain amount of ethylene; however, to provide ethylene hydroformylation, it is necessary to feed synthesis gas to the reactor (Fig. 1, flow I). The implementation of conversion processes using the membrane-assisted ethylene concentrating, oxycracking, and matrix-assisted conversion technologies leads to the formation of ethylene-enriched gas mixtures containing a fairly high amount of hydrogen and carbon monoxide (Fig. 1, flows II–IV); therefore, oxygen-containing compounds can be synthesized directly from the resulting gas mixtures, without constructing a separate plant for synthesis gas production [7–11]. The choice of the conversion method largely depends on the composition of the feed refinery gas.

It should be noted that saturated HCs are also formed in each of the above processes. There are published data on hydroformylation processes in media enriched in carbon dioxide or lower HCs (Gas Expanded Liquids, GXLs) [12–17]. It was reported that an increase in the total pressure in a hydroformylation reactor owing to gas supply contributes to a better saturation of the solvent with the reacting components—olefin, carbon monoxide, and hydrogen—and thereby has a positive effect on the reaction rate. The physicochemical constants of gases, such as critical temperature T_c and pressure P_c, determine the degree of expansion of the liquid phase. Under the reaction conditions (high pressures and temperatures), the expansion of the liquid phase volume owing to gas condensation can be 40–80% of the initial volume; therefore, the consumption of the solvent can be decreased. Using the example of the hydroformylation of propylene of the propane–propylene fraction, it was shown that the reactions in GXLs (using toluene, butanol-1, and NX-795 (butanal oligomer mixture) as

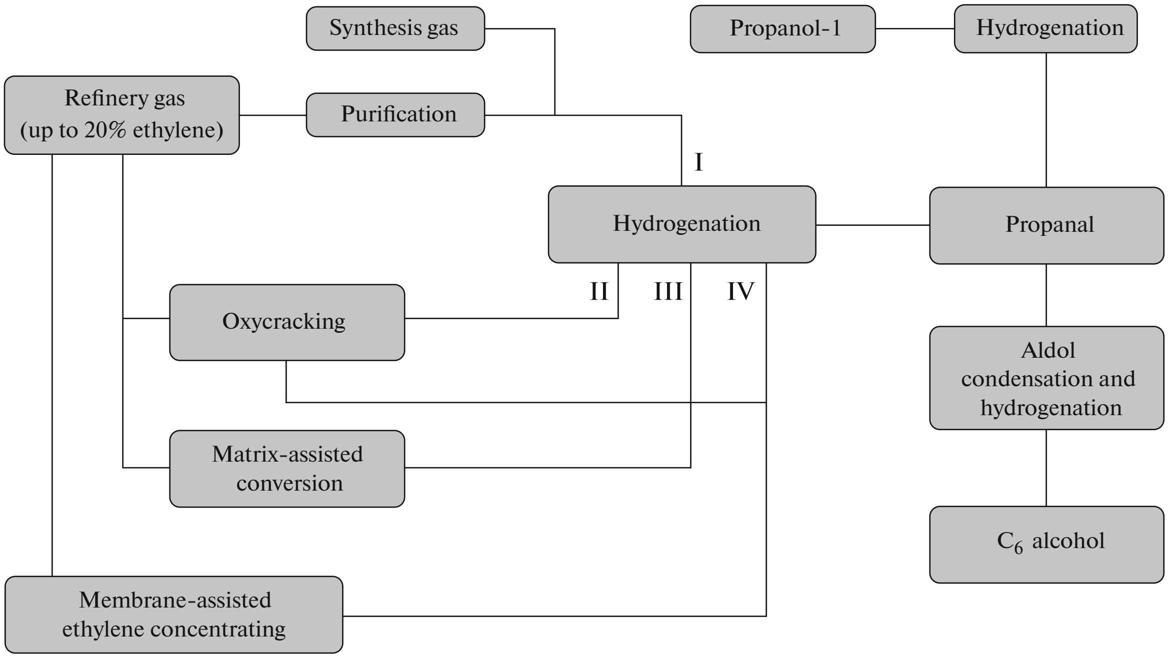

Fig. 1. Routes of the combined conversion of refinery gases.

solvents) exhibit a higher selectivity for linear aldehyde [12]. The implementation of the hydroformylation of propylene mixed with propane without the component separation stage is a more cost-effective process in terms of energy consumption; in this case, the propane-enriched stream from the hydroformylation reactor can be recycled to produce an additional amount of propylene. An advantage of the use of GXLs as alternative reaction media over the use of supercritical fluids is that gases should not be necessarily compressed to a high pressure [12].

This study is focused on the features of the ethylene hydroformylation reaction in gas mixtures enriched in saturated HCs (methane). The effect of the feed gas mixture composition, the initial pas pressure in the reactor, and temperature on the reaction rate and selectivity is studied. The catalyst system components are rhodium complexes with phosphine ligands, which make it possible to separate the catalyst from the reaction products by various methods.

EXPERIMENTAL

Triphenylphosphine trisulfonate (triphenylphosphine-3,3',3''-trisulfonic acid trisodium salt (TPPTS)), polyethylene glycol (M = 3000 g/mol), 4-(diphenylphosphino)benzoic acid, and 1,3-dicyclohexylcarbodiimide (Sigma-Aldrich) were used without further purification. The $Rh(acac)(CO)_2$ complex was synthesized as described in [18]. Solvents (toluene, acetylacetone) were prepared in accordance with standard procedures. Ethylene, hydrogen, methane, and carbon monoxide used in the study were purchased from Voessen.

Liquid products were analyzed by gas–liquid chromatography on a Khromos chromatograph equipped with a flame ionization detector and a 50-m-long capillary column coated with the SE-30 phase using temperature programming of 60–230°C, helium as a carrier gas, and n-heptane as an internal standard. Analysis by ^1H and ^{31}P nuclear magnetic resonance (NMR) spectroscopy was conducted on a VarianXL-400 instrument with an operating frequency of 400 MHz. Matrix-assisted laser desorption/ionization (MALDI) spectra were recorded on a Bruker Daltonics AutoflexII MALDI/time-of-flight mass spectrometer with a nitrogen laser at a working wavelength of 337 nm. The matrix was 2,5-dihydroxybenzoic acid.

Polyethylene Glycol (PEG)–PPh_3 Phosphine Ligand Synthesis Procedure

Initially, 0.5 g (1.62 mmol) of 4-(diphenylphosphino)benzoic acid and 5 mL of dichloromethane were placed in a round-bottomed flask equipped with a magnetic stirrer in an argon atmosphere. Twenty milligrams (0.16 mmol) of 4-dimethylaminopyridine and 2 g (0.67 mmol) of PEG (M = 3000 g/mol) were added to the solution under stirring. The mixture was cooled to 0°C; after that, 0.34 g (1.65 mmol) of 1,3-dicyclohexylcarbodiimide was added. The solution was stirred at 0°C for 5 min and then at room temperature for 3 h. Upon the completion of the reaction, the precipitate was filtered off on a paper filter and washed with dichloromethane. A tenfold excess of cooled diethyl ether was added to the filtrate; the resulting precipitate was filtered off on a glass-filter funnel in an argon atmosphere, washed three times with diethyl ether, and dried in an argon atmosphere. The resulting substance was a light yellow powder. The product yield was 1.9 g (85% of the theoretical yield).

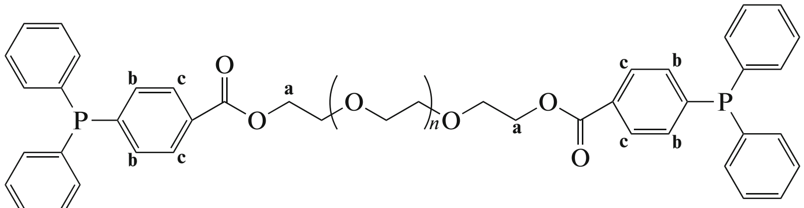

PEG-PPh$_3$

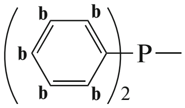

^1H NMR (400 MHz, $CDCl_3$) δ: 3.40–3.90 (m, 310H, $–(\mathbf{CH_2}–\mathbf{CH_2}–O)_n–$), 4.45 (m, 4H, H_a), 7.27–7.38 (m, 24H, H_b), 7.94–7.99 (m, 4H, H_c) ppm.

^{31}P NMR (162 MHz, $CDCl_3$) δ: –4.95 ppm.

Mass spectrum (MALDI): molecular mass distribution maximum $m/z = 3560$.

Table 1. Possible composition of gas mixtures supplied to the hydroformylation stage during the combined conversion of refinery gases

Component		Stream 1	Stream 2	Stream 3
H_2	Content, vol %	20.3	40.6	4.1
O_2		0.0	0.4	0.0
N_2		0.0	1.1	0.0
CO		10.4	12.6	6.6
CO_2		1.7	0.8	0.1
CH_4		43.3	25.1	41.2
C_2H_6		0.2	4.7	13.4
C_2H_4		5.9	12.0	25.5
C_2H_2		0.0	1.5	0.0
C_3H_8		0.0	0.5	1.7
C_3H_6		0.3	0.6	2.8
$\sum C_{4+}$		0.0	0.1	0.5

Table 2. Composition of the model gas mixtures

Model mixture no.	Component composition, vol %			
	C_2H_4	CO	H_2	CH_4
1	20	20	40	20
2	20	20	20	40
3	40	20	20	20

Catalytic Ethylene Hydroformylation Procedure

Reactions were run in a 25-mL ParrInstrument steel autoclave equipped with a mechanically driven stirring device (magnetic coupling), a gas-trapping stirrer, and a device for thermostating at temperatures of up to 350°C. The autoclave was charged with 4.0 mL of the solvent (toluene), catalyst system components—0.015 mmol of $Rh(acac)(CO)_2$ and 0.045 mmol (in terms of phosphorus) of the phosphine ligand,—and 0.6 mL of the internal standard (*n*-heptane). The autoclave was two times flushed with carbon monoxide and sequentially filled with methane to a predetermined pressure and then with carbon monoxide, hydrogen, and ethylene to predetermined pressures. The total pressure was controlled using the sensor of a Teledyne syringe pump. After that, stirring was turned on (1000 rpm); the autoclave was heated at a rate of 3°C/min and then held at a given temperature. Reaction was run under permanent stirring for a predetermined time, while recording the dependence of pressure and temperature on the reaction time. Upon the completion of the reaction, the autoclave was cooled to room temperature to record the readings of the pressure gage (error of 2 atm); after that, the autoclave was depressurized to take a sample for analysis.

RESULTS AND DISCUSSION

Table 1 shows examples of gas mixtures from combined refinery gas conversion units. The composition of the product gas mixture depends on the feed refinery gas composition (methane, fatty gas, and olefin concentrations), the selected combined conversion route, and partial oxidation conditions, such as the residence time of the feedstock in the reactor, temperature, pressure, and feedstock consumption rate [7, 19].

The implementation of the operating mode of the combined units (Fig. 1) makes it possible to control the composition of the gas mixtures supplied to the oxosynthesis stage. Therefore, the hydroformylation of model mixtures listed in Table 2 was studied. Meth-

Table 3. Comparison of the physicochemical parameters of lower HCs

Gas	Physicochemical constants		Measurement conditions	Expansion, $V(T,P)/V_0$	Reference
	T_c, °C	P_c, atm			
CO_2	31.0	73.8	40°C, 20 atm	1.45	[14]
Methane	−83.7	42.6	Not available		
Propane	96.6	42.5	80°C; 12 atm	1.4	[12]
Butane	152.0	37.0	160°C; 70 atm	1.4	[13]

ane was used as saturate HC component. Table 3 shows the physicochemical constants of gases that were previously used as media to study the hydroformylation of olefins.

Depending on T_c and P_c of gases, the liquid (solvent) can expand owing to the absorption of the gases; the relative expansion of the liquid (V/V_0) depends on the gas pressure and temperature. To generate GXLs, it is advantageous to use gases whose critical temperature is slightly lower than the temperature of the studied reaction [12, 13]. Data in Table 3 suggest that, in the case of methane, a significant saturation and expansion of the liquid is scarcely probable. However, since the presence of methane in the system leads to an increase in the total pressure, the dissolution of gaseous reactants (C_2H_4, CO, and H_2) in toluene, along with their contact with the homogeneous catalytic complex, is more effective.

Currently, about 50% of all industrial oxosynthesis processes are implemented using modified rhodium–phosphine complexes; the reaction products (aldehydes) are separated from the catalyst solution by the distillation method. Alternative methods for the separation and recycling of catalyst systems are based on the use of water-soluble ligands in two-phase systems, temperature-controlled ligands, and ionic liquids and the separation of the catalytic complex by extraction and membrane nanofiltration processes [20–23]. The catalyst systems used in this study comprised a catalyst precursor—rhodium complex $Rh(acac)(CO)_2$—and phosphine ligands providing the isolation of catalyst systems from reaction mixtures by various methods.

A general scheme to describe possible chemical conversions during hydroformylation is shown below.

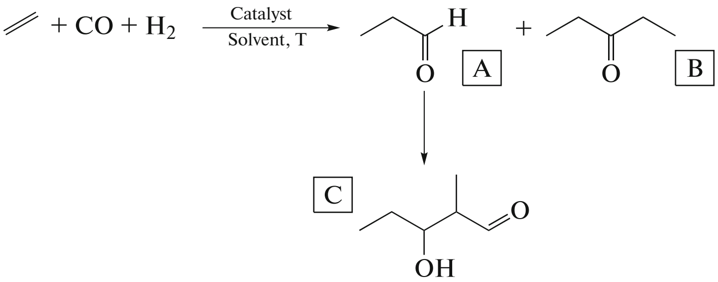

Schematic hydroformylation of ethylene.

The reaction results in the formation of propanal (A), diethyl ketone (B), and aldol (C).

Using the example of the hydroformylation of model mixtures 1–3 in the presence of a classical Rh/PPh_3 catalyst system, the effect of the total initial pressure and reaction temperature was studied. In the study, the absorption rate of gaseous components—ethylene (substrate, S), CO, and H_2—was determined form the pressure drop in a stationary reactor under uniform heating from room temperature to a given temperature. The kinetics of ethylene and propylene hydroformylation reactions in the presence of rhodium catalysts was studied in detail in [24, 25]; therefore, the aim of this study was to obtain data on the effect of saturated HC components and the composition of model gas mixtures on ethylene conversion. Figure 2 shows the reaction profile for the hydroformylation of model mixture 1 (dependence of the gas pressure in the reactor on the reaction time) at an initial gas pressure of 100 atm under heating from 25 to 80°C at a rate of 3°C/min. The figure also shows a thermal expansion curve of methane (dotted line), which characterizes the pressure in the reactor provided that the reaction and gas absorption do not occur.

A temperature of 55°C corresponds to the onset of the reaction; an almost complete absorption of the gaseous components is achieved by the time at which the reaction mixture is heated to 80°C. The efficiency of the catalyst system (turnover frequency (TOF), h^{-1}) for the curve portion that describes the most rapid

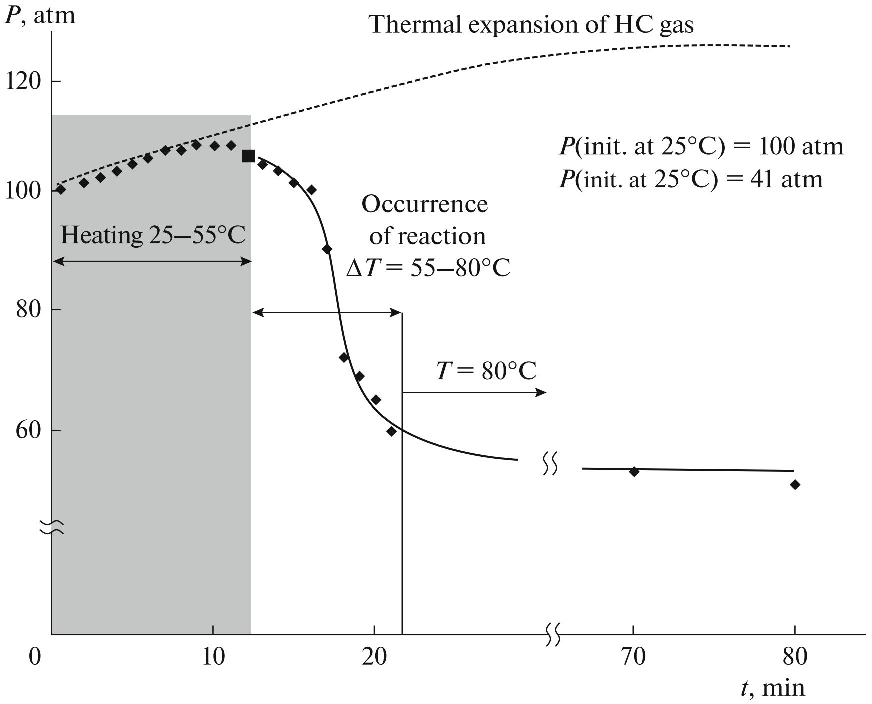

Fig. 2. Reaction profile for the hydroformylation of model mixture 1. Reaction conditions: $Rh(acac)(CO)_2$, 4 mg; PPh_3, 12 mg; S/Rh = 1600; toluene, 4 mL; heptane, 0.6 mL; P_{init} = 100 atm; heating rate, 3°C/min; and T_{fin} = 80°C.

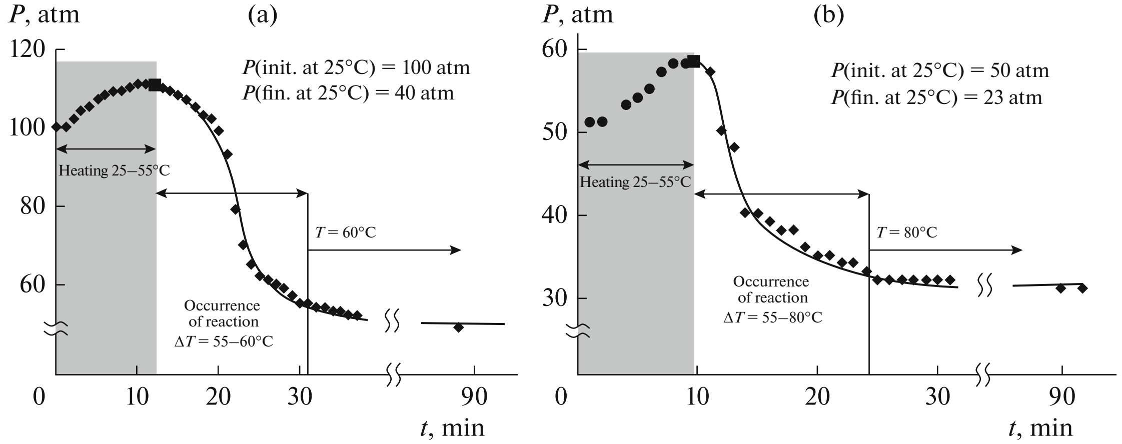

Fig. 3. Reaction profile for the hydroformylation of model mixture 1: (a) at a temperature of 60°C, an initial pressure of 100 atm, and S/Rh = 1600 and (b) at a temperature of 80°C, a pressure of 50 atm, and S/Rh = 800. Reaction conditions: $Rh(acac)(CO)_2$, 4 mg; PPh_3, 12 mg; toluene, 4 mL; heptane, 0.6 mL; and heating rate, 3°C/min.

occurrence of the reaction was 9500 h^{-1}; it was determined by formula (1):

$$\mathrm{TOF} = \frac{n\ (\text{reacted ethylene})}{n(\mathrm{Rh})t_{\text{reaction}}}. \tag{1}$$

The amount of reacted ethylene (in mol) was determined by the equation of state for gases using the residual pressure values. The formation of a single product—propanal (A)—was recorded; the amount of this product corresponds to the stoichiometric reaction. In this case, the formation of the hydrogenation product—ethane—is negligible and scarcely probable because the threshold of activation energy for the hydrogenation reaction is higher than that for the hydroformylation reaction [25]. The reaction rate significantly decreases, while the gaseous reagents are consumed and their residual concentrations become low; however, the reaction occurs to nearly complete conversion of the gaseous reagents; the presence of methane in the system contributes to a better dissolu-

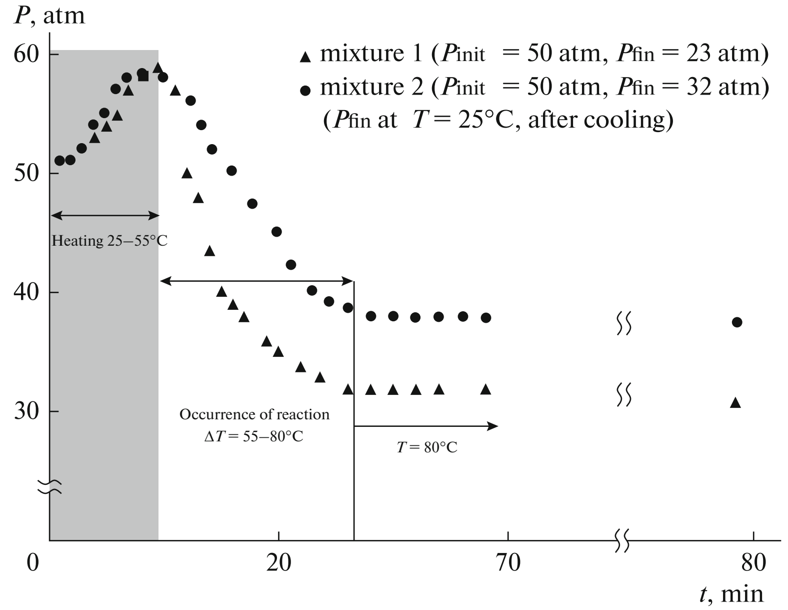

Fig. 4. Reaction profile for the hydroformylation of model mixtures 1 and 2. Reaction conditions: $Rh(acac)(CO)_2$, 4 mg; PPh_3, 12 mg; S/Rh = 800; toluene, 4 mL; heptane, 0.6 mL; $P_{init} = 50$ atm; heating rate, 3°C/min; and $T_{fin} = 80$°C.

tion of the gases and their transfer to the active sites of the catalyst.

Figures 3a and 3b show reaction profiles for the hydroformylation of model mixture 1 (a) at a temperature of 60°C and an initial pressure of 100 atm and (b) at 80°C and an initial pressure of 50 atm.

A decrease in the final reaction temperature from 80 to 60°C leads to an increase in the complete ethylene conversion time (TOF = 6000 h^{-1}) and the formation of a diethyl ketone–propanal mixture in a ratio of 1 : 10. The implementation of a similar reaction with holding of the reaction medium at a final temperature of 120°C contributes to the occurrence of aldol condensation to form aldol (C); the aldol content in the final mixture achieves 48%. With a decrease in the initial pressure of mixture 1 fed to the reactor to 50 atm, the reaction profile and selectivity vary only slightly.

The hydroformylation of model mixtures 1 and 2 made it possible to determine the effect of excess hydrogen on the reaction rate and selectivity (Fig. 4).

Excess hydrogen contributes to an increase in the reaction depth and the propanal selectivity (up to 99%). The residual pressure of gas mixture 2 (methane-enriched) was 32 atm, 20 atm of which are accounted for the pressure of methane and the remaining 12 atm are attributed to the pressure of a gas mixture of ethylene with carbon monoxide and hydrogen; 20% of diethyl ketone and 80% of propanal were identified in the products. The more gently sloping gas pressure variation curve in the hydroformylation of gas mixture 2 also suggests that, for the mixture that is not enriched in hydrogen, the reaction rate is lower, although an identical temperature is required for the onset of the reaction in the two cases.

Model mixture 3 represents an approximate composition of industrial gas mixtures enriched in ethylene; these mixtures contain ethylene in excess relative to the amount of both carbon monoxide and hydrogen. In the study, the hydroformylation of model mixture 3 was run in the presence of the rhodium–phosphine catalyst ($Rh(acac)(CO)_2 + PPh_3$) in toluene at temperatures of 60 and 80°C (Table 4). In this case, in addition to propanal, diethyl ketone was formed (15 and 20%, respectively).

Table 4. Hydroformylation of model mixture 3 at temperatures of 60 and 80°C*

T, °C	P_{init}, atm	P_{fin}, atm	Ethylene conversion, %	Reaction selectivity, %		TOF, h^{-1}
				propanal (A)	diethyl ketone (B)	
60	75	40	78	85	15	3700
80	75	35	90	80	20	6500

* Reaction conditions: $Rh(acac)(CO)_2$, 4 mg; PPh_3, 12 mg; S/Rh = 2400; toluene, 4 mL; heptane, 0.6 mL; and heating rate, 3°C/min.

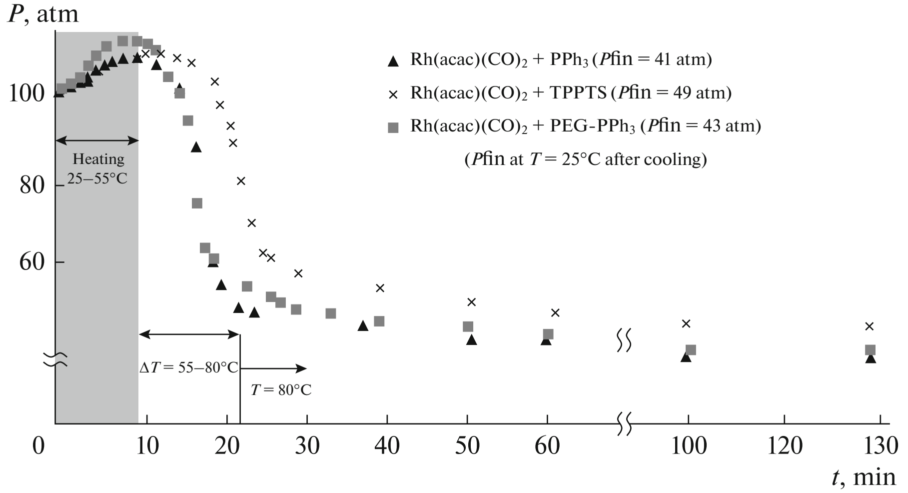

Fig. 5. Reaction profile for the hydroformylation of model mixture 1 with different ligands. Reaction conditions: $Rh(acac)(CO)_2$, 4 mg (0.015 mmol); ligand, 0.045 mmol; S/Rh = 1600; toluene, 4 mL; heptane, 0.6 mL; $P_{init} = 50$ atm; heating rate, 3°C/min; and $T_{fin} = 80$°C.

The experimental data on the hydroformylation of model mixtures 1–3 suggest that industrial gas mixtures enriched in inert HCs (in particular, methane) can be converted to various oxygenates by hydroformylation in the presence of a rhodium–phosphine catalyst; in this case, acceptable reaction rates and propanal selectivities are achieved at reaction temperatures of 60–80°C and initial pressures of the gas mixture of 50–100 atm. The steepest portions of the gas absorption curves correspond to the efficiency of the catalyst system with a TOF value of 3500–9500 h^{-1}. In the described examples, a homogenous catalyst can be separated from the reaction products only by the distillation method, which has some known disadvantages; therefore, the hydroformylation of model mixture 1 was studied using phosphine ligands providing the isolation of the catalyst system from homogeneous media by alternative methods; the ligands are shown below.

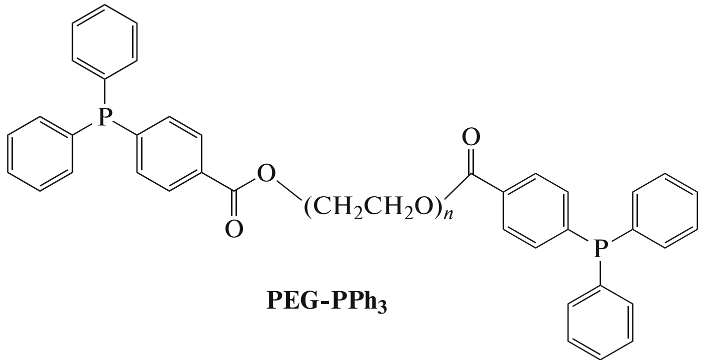

PEG-PPh$_3$

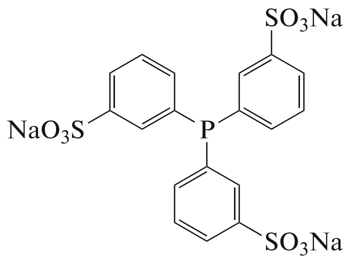

TPPTS

Polyethylene glycol–PPh_3 is a macromolecular ligand synthesized by modifying PEG with an average molecular mass of 3000 g/mol; TPPTS is sodium triphenylphosphine trisulfonate. It was previously found [26] that the PEG–PPh_3 macromolecular ligand can be isolated from the reaction medium by nanofiltration using membranes whose pore size does not exceed 2 nm. It is known that TPPTS is a water-soluble ligand; using TPPTS, hydroformylation is implemented in a water–organic solvent two-phase system [27].

Figure 5 shows comparison of the reaction profiles in the presence of the different catalyst systems. In the case of TPPTS, the onset of the reaction is slightly shifted to the region of higher temperatures (onset of the reaction at $T \approx 70$°C); at low reactant concentrations, the decrease in the rate is more significant than that in the case of PPh_3 and PEG–PPh_3. This finding can be attributed to the presence of water in the system and the fact that the catalyst is in the aqueous phase. The solubility of the reactants in this system is lower than that in pure toluene; the rate-limiting step can be the reactant transfer to the interface, where the catalytic reaction occurs. The variation in the ligand does not affect the reaction selectivity; in each case, propanal was identified as the main product in the liquid phase (98–99%).

Table 5. Correlation of catalyst systems and hydroformylation methods

Catalyst system	Process	Catalyst separation and recycling	Prototype
Rh/PPh_3	Continuous-running	Distillation, recycling of the catalyst solution stream	[28]
Rh/PEG–PPh_3		Nanofiltration	[29]
Rh/TPPTS		Phase separation	[30]

CONCLUSIONS

In the studies, optimum conditions for the hydroformylation of ethylene-containing gas mixtures enriched in HC gases have been determined. The studied catalyst systems can be correlated (Table 5) with a process in which this stage of the combined conversion of refinery gases to oxygenates can be implemented with the highest efficiency and the lowest costs. It has been found that, in the hydroformylation of hydrogen-enriched mixtures in the presence of rhodium–phosphine catalysts, propanal is formed as the main product (up to 99%), while the formation of diethyl ketone (up to 20%) occurs if ethylene is present in the mixture in a molar excess relative to CO.

FUNDING

This work was supported by the Ministry of Education and Science of the Russian Federation (grant agreement no. 14.607.21.0171, identifier RFMEFI60717X0171).

REFERENCES

1. J. A. Melero, J. Iglesias, and A. Garcia, Energy Environ. Sci. **5**, 7393 (2012).
2. X. B. Luo, M. H. Wang, X. G. Li, et al., Fuel **158**, 424 (2015).
3. X. G. Li, Y. Li, L. H. Zhang, and H. Li, Chem. Eng. Res. Des. **109**, 258 (2016).
4. D. N. Gorbunov, M. V. Terenina, Yu. S. Kardasheva, et al., Pet. Chem. **57**, 1137 (2017).
5. D. L. Wang and X. Feng, Int. J. Hydrogen Energy **38**, 12968 (2013).
6. A. V. Nikitin, I. V. Sedov, A. V. Ozerskii, et al., in *Proceedings of XII International Conference of Young Scientists on Petroleum Chemistry, September 17–21, 2018, Zvenigorod, Russia*, Book of Abstracts, p. 531.
7. R. N. Magomedov, A. V. Nikitin, V. I. Savchenko, and V. S. Arutyunov, Kinet. Catal. **55**, 556 (2014).
8. V. S. Arutyunov, V. I. Savchenko, I. V. Sedov, et al., Chem. Eng. J. **282**, 206 (2015).
9. V. S. Arutyunov, V. I. Savchenko, I. V. Sedov, et al., Russ. J. Appl. Chem. **89**, 1816 (2016).
10. A. V. Nikitin, A. V. Ozerskii, K. A. Timofeev, et al., Gorenie Vzryv **11** (2), 18 (2018).
11. C. Hu, J. Wu, H. Zhang, and S. Qin, AIChE J. **53**, 2925 (2007).
12. D. Liu, V. R. Chaudhari, and B. Subramaniam, Chem. Eng. Sci. **187**, 148 (2018).
13. D. Liu, Z. Xie, W. K. Snavely, et al., React. Chem. Eng. **3**, 344 (2018).
14. H. Jin and B. Subramaniam, Chem. Eng. Sci. **59**, 4887 (2004).
15. D. Liu, V. R. Chaudhari, and B. Subramaniam, AIChE J. **64**, 970 (2018).
16. B. Subramaniam, V. R. Chaudhari, S. A. Chaudhari, et al., Chem. Eng. Sci. **115**, 3 (2014).
17. M. Caporali, P. Frediani, F. Piacenti, and A. Salvini, J. Mol. Catal., A **204–205**, 195 (2003).
18. Yu. Varshavskii and T. Cherkasova, Neftekhimiya **12**, 1709 (1967).
19. A. V. Ozerskii, A. V. Nikitin, I. V. Sedov, et al., Russ. J. Appl. Chem. **91**, 2065 (2018).
20. A. Börner and R. Franke, *Hydroformylation: Fundamentals, Processes, and Applications in Organic Synthesis* (Wiley–VCH, Weinheim, 2016), Vol. 1.
21. D. N. Gorbunov, A. V. Volkov, Yu. S. Kardasheva, et al., Pet. Chem. **55**, 587 (2015).
22. T. Rosler, T. Fassbach, M. Schrimpf, et al., Ind. Eng. Chem. Res. **58**, 2421 (2019).
23. J. Marinkovic, A. Riisager, and R. Franke, Ind. Eng. Chem. Res. **58**, 2409 (2019).
24. S. N. Rush, Yu. G. Noskov, T. E. Kron, and G. A. Korneeva, Kinet. Catal. **50**, 557 (2009).
25. G. Kiss, E. G. Mozeleski, K. C. Nadler, et al., J. Mol. Catal., A **138**, 155 (1999).
26. D. S. Safronova, D. N. Gorbunov, and E. A. Karakhanov, in *Proceedings of XII International Conference of Young Scientists on Petroleum Chemistry, October 18–21, 2018, Zvenigorod, Russia*, Book of Abstracts, p. 235.
27. I. Horváth, R. V. Kastrup, A. Oswald, and A. E. Mozeleski, Catal. Lett. **2**, 85 (1989).
28. V. A. Rybakov, A. L. El'kin, G. N. Tyukavin, et al., *Technology of Oxosynthesis and Related Processes Involving Carbon Monoxide* (Sibur-Khimprom, Perm, 2004) [in Russian].
29. B. Cornils, R. W. Fischer, and C. Kohlpaintner, Butanals, in *Ullmann's Encyclopedia of Industrial Chemistry* (Wiley–VCH, New York, 2000). https://doi.org/10.1002/14356007.a04_447
30. A. Lejeune, M. Rabiller-Baudry, T. Renouard, et al., *Chem. Eng. Sci.* **183**, 240 (2018).

Translated by M. Timoshinina